Atlantic Multidecadal Oscillation modulates the impacts of Arctic sea ice decline

Fei LI [*1,2], Yvan J. ORSOLINI [1,3], Huijun WANG [2,4,5], Yongqi GAO [6,5], and Shengping HE [7]

[1]*NILU – Norwegian Institute for Air Research, Kjeller 2007, Norway*

[2]*Collaborative Innovation Center on Forecast and Evaluation of Meteorological Disasters/Key Laboratory of Meteorological Disaster, Ministry of Education, Nanjing University of Information Science and Technology, Nanjing 210044, China*

[3]*Bjerknes Center for Climate Research, Bergen 5007, Norway*

[4]*Climate Change Research Center, Chinese Academy of Sciences, Beijing 100029, China*

[5]*Nansen-Zhu International Research Centre, Institute of Atmospheric Physics, Chinese Academy of Sciences, Beijing 100029, China*

[6]*Nansen Environmental and Remote Sensing Center, Bergen 5006, Norway*

[7]*Geophysical Institute, University of Bergen, Bergen 5007, Norway*

* Corresponding author: lifei-715@163.com

This article has been accepted for publication and undergone full peer review but has not been through the copyediting, typesetting, pagination and proofreading process which may lead to differences between this version and the Version of Record. Please cite this article as doi: 10.1002/2017GL076210

Abstract

The Arctic sea ice cover has been rapidly declining in the last two decades, concurrent with a shift in the Atlantic Multi-decadal Oscillation (AMO) to its warm phase around 1996/97. Here we use both observations and model simulations to investigate the modulation of the impacts of the decreased sea ice cover in the Atlantic sector of the Arctic (AASIC) by the AMO. We find that the AASIC loss during a cold AMO phase induces increased Ural blocking activity, a southeastward-extended snowpack and a cold continent anomaly over Eurasia in December through northerly cold air advection and moisture transport from the Arctic. The increased Ural blocking activity and more-extended Eurasian snowpack strengthen the upward propagation of planetary waves over the Siberian–Pacific sector in the lower stratosphere and hence lead to a weakened stratospheric polar vortex and a negative Arctic Oscillation (AO) phase at the surface in February. However, corresponding to the AASIC loss during a warm AMO phase, one finds more widespread warming over the Arctic and a reduced snowpack over Northern Eurasia in December. The stratosphere–troposphere coupling is suppressed in early winter and no negative AO anomaly is found in February. We suggest that the cold AMO phase is important to regulate the atmospheric response to AASIC decline and our study provides insight to the ongoing debate on the connection between the Arctic sea ice and the AO.

Key Points:

- The AASIC loss during a cold AMO phase favors increased Ural blockings, a southeastward-extended snowpack and cold Eurasia in December.
- The anomalous blockings and snowpack weaken the stratospheric polar vortex via vertical wave propagation, with a negative AO in February.
- The AASIC loss during a warm AMO phase does not exhibit cold Eurasia in December, nor a significant negative AO in February.

1. Introduction

The Arctic sea ice cover has diminished at a striking rate in the past decades, in all seasons but most strongly in summer and autumn, concurrent with a pronounced Arctic surface warming [*Stroeve et al.,* 2012]. At the same time, observations show decreased surface air temperature (TS) over Eurasia in winter [*Honda et al.,* 2009; *Cohen et al.,* 2012; *Mori et al.,* 2014; *Kug et al.,* 2015], termed as "Warm Arctic, Cold Eurasia" [*Cohen et al.,* 2013, 2014]. The Arctic sea ice loss has also been linked to an increase in the snowpack over parts of Eurasia as a result of increased moisture source over ice-free Arctic seas and tropospheric moisture transport [*Li et al.,* 2012; *Liu et al.,* 2012; *Wegmann, et al.,* 2015]. The large-scale variability in the extratropical TS is closely related to changes in the position of storm tracks and jet stream [*Francis and Vavrus,* 2012], which is largely controlled by the dominant atmospheric modes of variability such as the Arctic Oscillation (AO). It has hence been suggested that the late-winter atmospheric response to the decreased sea ice in early-winter over the Barents-Kara Seas reflects a negative phase of the AO, and the underlying mechanisms are related to the upward propagation of planetary waves into the stratosphere [*Li et al.,* 2012; *Peings and Magnusdottir,* 2014; *Kim et al.,* 2014; *King et al.,* 2016; *Zhang et al.,* 2016; *Screen,* 2017]. On the other hand, some studies pointed out that the winter atmospheric response to Arctic sea ice decrease does not robustly display a negative AO signature [e.g., *Liu et al.,* 2012; *Smith et al,* 2017]. *Mori et al.* [2014] argued that the winter atmospheric response to Arctic sea ice anomaly is an intensification of the Siberian High, which is approximately independent of the AO. Hence, whether the observed "Warm Arctic, Cold Eurasia" pattern can be causally attributed to sea ice reduction remains debated. In model studies, it has been proposed to arise purely from natural internal variability [*McCusker et al.,* 2016; *Sun et al.,* 2016]. The modelled mid-latitude atmospheric responses to the decline of sea ice are less certain in terms of robustness, pathway and magnitude [*Vihma,* 2014; *Gao et al.,* 2015], and might also depend on the background climatic state [*Balmaseda et al.,* 2010; *Overland et al.,* 2016; *Smith et al.,* 2017].

There is evidence that the Arctic sea ice cover has varied substantially on interannual, decadal and multi-decadal timescales [*Day et al.,* 2012]. The shift in the Atlantic

Multi-decadal Oscillation [AMO; *Schlesinger and Ramankutty,* 1994], accompanied by anomalous oceanic heat transport toward the Arctic, is relevant for sea ice multi-decadal variability, especially in the Atlantic sector of the Arctic [*Årthun et al.*, 2012; *Miles et al.*, 2014; *Onarheim et al.*, 2014; *Zhang*, 2015]. *Osborne et al.* [2017] recently showed that the AMO phase can modulate the impact of Arctic sea ice loss on the horizontal wave propagation in winter, with Arctic sea ice loss associated to a trough–ridge–trough response over the Pacific–North America only during a cold AMO phase (AMO−). Moreover, the AMO can regulate the frequency of atmospheric blocking highs over the Euro–Atlantic sector by changing the baroclinicity and transient eddy activity [*Häkkinen et al.*, 2011; *Peings and Magnusdottir,* 2014; *Omrani et al.*, 2014, 2016]. The increased (reduced) blocking highs over the Euro–Atlantic sector can further enhance (weaken) the vertical wave propagation, resulting a weakened (strengthened) stratospheric polar vortex [*Nishii et al., 2011; Li et al., 2018*].

However, the AO is responding to many drivers in a season-dependent fashion [*Gao et al.*, 2015]. In particular, both observational [*Saito et al.*, 2001] and modeling [*Gong et al.*, 2003; *Orsolini et al.*, 2009; *Peings et al.*, 2012] studies also suggest that the late autumn Eurasian snowpack also has a strong effect on the AO and the stratosphere–troposphere interactions in winter. Through thermodynamical and radiative effects, a thicker Eurasian snowpack strengthens the vertical wave propagation in proximity to the high topography of Asia, and hence induces a weakened stratospheric polar vortex and a negative AO phase at the surface [*Cohen et al.*, 2007; *Orsolini et al.*, 2016]. *Orsolini et al.* [2013] showed that the increase in early winter Eurasian snowpack can also induce a "Warm Arctic, Cold Eurasia" pattern through surface thermal forcing and intensification of the Siberian High and poleward heat transport.

In this paper, we demonstrate with both reanalyses and numerical simulations that the impacts of Arctic sea ice decline on the wintertime stratosphere–troposphere coupling and on the AO at the surface are modulated by the phase of the AMO, and that the Eurasian snowpack plays a role in that linkage.

2. Data and Methods

2.1 Observational Data and Model Experiments

We have used monthly mean and daily datasets the European Centre for Medium-Range Weather Forecasts (ECMWF) Twentieth Century Reanalysis [ERA20C; 1900–2010; *Poli et al.,* 2016] and ECMWF Interim Reanalysis [ERA-I; 1979–2017; *Dee et al.,* 2011]. Sea ice concentration from the Hadley Centre Sea Ice and sea surface temperature (SST) dataset version 2 [HadISST2; 1850–2017; *Titchner and Rayner,* 2014], and snow depth from ERA-I/Land [1980–2015; *Balsamo et al.,* 2015] are also used. We focus mainly on the satellite era (1979/80–2016/17), since the available sea ice observations prior to the satellite era are quite limited both spatially and temporally, and presumably subject to a large uncertainty [*Johannessen et al.,* 2004]. Some recent studies re-calibrated long-term time series of Arctic sea ice cover based on the National Snow and Ice Data Center [NSIDC; 1850–2013; *Walsh et al.,* 2017] and "Russian" [1900–2008; *Mahoney et al.,* 2008] sea ice datasets and Arctic TS records [*Connolly et al.,* 2017], and have had success in reproducing the sea ice multi-decadal variations. However, the interannual variability of sea ice prior to the satellite era shows an apparent diversity in different datasets. Nevertheless, we also tested the robustness of our conclusions using the long-term NSIDC sea ice record, given the above-mentioned caveat.

To further investigate the response to sea ice changes under different phases of the AMO, we also utilized a set of 10-member ensemble experiments carried out with the same ECMWF atmospheric model as used in producing the ERA20C reanalysis [ERA20CM; 1900–2010; *Hersbach et al.,* 2015]. The ERA20CM run was driven by the HadISST2 SST and sea ice concentration with radiative forcing from the Coupled Model Intercomparison Project Phase 5, hence with the same sea surface boundary conditions and radiative forcing as ERA20C, but does not assimilate any observations, in contrast to ERA20C (Table S1).

2.2 Climatic Indices and Methods

The smoothed AMO index [with a 121-month smoother; 1861–2011; *Enfield et al.,* 2001] is provided by NOAA's Earth System Research Laboratory, Physical Sciences Division. The AMO− and AMO+ (warm AMO phase) correspond to cases in which the smoothed AMO index is above and below zero, respectively. We define the Atlantic Arctic sea ice cover

(AASIC) index based upon the area weighted average of sea ice concentration anomalies over (72°–85°N, 20°W–90°E). Our analysis focuses on December, when the AASIC index has larger interannual variations over the southern Barents Sea than that in October and November, which makes it more relevant to the winter atmospheric circulation anomalies in both the troposphere and stratosphere (Fig. S1).

To isolate the influence of sea ice loss on the interannual timescale, linear trends have been removed for each period (e.g., during the AMO−, AMO+, or a longer period irrespective of the AMO phase) prior to analysis from the AASIC index and all the fields. The wave activity flux is used to identify the origin and propagation of Rossby wave-like perturbations [*Plumb,* 1985]. Blocking high events are defined as intervals in which daily 500 hPa height exceeds one standard deviation above the monthly mean for each grid cell over five consecutive days [*Thompson and Wallace,* 2001; *Liu et al.*, 2012; *Tang et al.*, 2013]. The local frequency of blocking is measured as the ratio between the number of blocked days and the total number of days. The statistical significance of the correlation is assessed using a two-tailed Student's *t* test.

3. Results

The smoothed December–February mean AMO index exhibits a period of roughly 60–70 years (Fig. 1a). Over the 1979–1995 (1996–2016) period under the AMO− (AMO+), there is above-normal (below-normal) December AASIC (Fig. 1b: red bar). The decadal difference of the standard deviation of sea ice concentration between 1979–1995 and 1996–2016 shows larger interannual variations of December AASIC over the Greenland and southern Barents Seas and smaller interannual variations to the northern Barents Sea and east of Novaya Zemlya (Fig. 1c). Given that there exists a strong interannual variability in AASIC during both the AMO+ and AMO− (Fig. 1b: black line), we will explore whether the impact of AASIC decline onto the atmosphere depends on the phase of the AMO.

3.1 Modulation by the AMO in ERA20C

While we will examine the modulation of the interannual sea ice impact by the AMO in the satellite era, we begin by showing how the decadal variability associated with the AMO

influences the atmospheric variables in ERA20C over the whole twentieth century. The composite difference of the vertical component of December 150-hPa stationary wave activity flux (F_Z) (the AMO− minus the AMO+) shows anomalous downward (upward) 150-hPa F_Z over the North Atlantic and Western Russia (Southern Europe, East Asia and the eastern North Pacific) (Fig. 2a). The simultaneous blocking activity is reduced over the Euro–Atlantic sector as in *Häkkinen et al.* [2011], which might lead to an intensification of the upper-tropospheric polar vortex via the anomalous downward 150-hPa $F_{Z,}$ and hence to an accumulation of cold air over the Arctic (Figs. 2b, 2d, S2a). The composite difference also reveals a thicker snowpack over Western Russia and Northern Europe associated with a cyclonic sea level pressure (SLP) anomaly west of the Urals (Figs. 2c, 2d). Furthermore, the December zonal wave (wavenumber 1) along 40°N is intensified from the surface to the lower stratosphere (Fig. S3a). This suggests an enhanced vertical wave propagation into the stratosphere over the AMO− period. In February, the AMO− is associated with a deeper and eastward-extended Aleutian Low (Fig. 2e), consistent with previous studies [*Dima and Lohmann,* 2007; *Li et al.,* 2018].

3.2 Influence of AASIC decline on the AO during different AMO phases

We now consider the influence of AASIC decline during both the AMO− and AMO+ in ERA-I. The regression of December 150-hPa F_Z upon the negative AASIC index during the AMO− shows anomalous upward 150-hPa F_Z over the Siberian–Pacific sector (Fig. 3a). The increased blocking activity is seen over the Urals and the Barents Sea, concurrent with an enhanced high over the Urals and a thicker (below-normal) snowpack in Central Asia, Southern Siberia, and the Far East (Northern Siberia) (Figs. 3b, 3c, S2b). On one hand, the northerly cold air advection and moisture transport along the eastern and southern flanks of the enhanced Ural High favor a thicker, southeastward-extended snowpack and a cold continental anomaly over Eurasia (Figs. 3c, 3d), consistent with *Wegmann et al.* [2015]. On the other hand, the more-extended snowpack can induce a zonally asymmetric temperature distribution, with a cold anomaly over the snow-covered Central Asia and Southern Siberia. The asymmetric temperature distribution in turn favors more Ural blockings [*García-Herrera and Barriopedro,* 2006]. We also find an anomalous mid-latitude wave train over the

Pacific–North American sector in December (Fig. S2b), consistent with *Overland et al.* [2016]. In February, the SLP pattern shows resemblance to the negative AO phase, with centers of action over the Pacific, Atlantic and Arctic (Fig. 3e). Notably, the anomalous stratospheric wave-driving leads to a positive Arctic height anomaly in the stratosphere in December, indicative of a weaker polar vortex, which subsequently propagates down to the surface in February (Fig. S4a).

By comparison, during the AMO+, the AASIC loss is associated with anomalous downward 150-hPa F_Z over Siberia, a below-normal snowpack over Northern Eurasia and more widespread warming over the Arctic in December (Figs. 3f, 3h 3i). There is little change in blocking activity, except for a localized decrease around the Caspian Sea, nor a clear negative AO pattern in February (Fig. 3g, 3j), contrary to the AMO− case.

3.3 Role of Eurasian snow depth in AASIC–Stratosphere Coupling

The results mentioned above indicate the potential positive feedback between the increased Ural blocking activity and the thicker, more-extended Eurasian snowpack, which both can enhance the vertical propagation of planetary waves into the stratosphere. We further investigate the role of Eurasian snow depth (ESD) by showing the regressions of geopotential height anomaly averaged between 40°–50°N upon the ESD index. During the AMO−, the anomalous zonal wave is nearly in phase with the climatological wavenumber 1, except for a minimum over 90°E (Fig. S3b). The southeastward-extended Eurasian snowpack favors the vertical wave propagation into the stratosphere in December. However, during the AMO+, the anomalous zonal wave is out of phase with the climatological wavenumber 1 (Fig. S3c), suggesting a suppressed vertical wave propagation in December. Hence, the location in longitude of ESD-related geopotential height anomaly is important for the constructive interference with the background planetary wavenumber 1 during the AMO−, while during the AMO+, the interference is destructive. In other words, the AASIC loss induces an enhanced vertical wave propagation into the stratosphere in December only during the AMO−, in conjunction with a more-extended Eurasian snowpack (Figs. S3d, S3e).

The scatter plots (Fig. S5) clearly indicate significant linear relationships among December AASIC, ESD, 150-hPa F_Z and February AO indices during the AMO−. The

correlation coefficient between December AASIC and December 150-hPa F_Z (February AO) is −0.50 (0.61), and the one between December ESD and 150-hPa F_Z is 0.49. However, there are no significant correlations during the AMO+.

3.4 Model Simulations

We next return to the evaluation of the decadal impacts of the AMO in the ERA20CM simulations (Fig. 2: right panel). The composite difference shows an anomalous downward 150-hPa F_Z over Western Russia, reduced blocking activity over the Euro–Atlantic sector and a thicker snowpack over Western Russia and Northern Europe in December, as well as deeper Aleutian Low in February. However, the simulated cyclonic SLP anomaly in December is located further south as compared with ERA20C. The associated northerly cold air advection and moisture transport spill southward along the western flank of the cyclonic SLP anomaly, and the simulated warm continental anomaly over the mid-latitude Eurasia is weaker (Figs. 2h, 2i) than that in ERA20C.

The influence of the AMO phase on the AASIC-related extratropical stratosphere–troposphere coupling is now explored by performing a regression analysis of the ERA20CM simulations (Fig. 4), as was done with ERA20C. For the combination of the AASIC loss and AMO−, the model simulations reproduce the anomalous upward 150-hPa F_Z over the North Pacific and Central Eurasia, but an anomalous downward one over Arctic Eurasia (Fig. 4a) contrary to the reanalysis. The ERA20CM-based regressed anomalies display increased blocking activity over and east of the Urals, a thicker snowpack over Central Eurasia, a cold continental anomaly over Asia and Russia in December and a negative AO phase in February, albeit weaker than that in the reanalysis. It is worth noting that the simulations fail to capture the increased blocking activity over the Barents Sea, the thicker snowpack over the Far East, and the northerly moisture transport from the Arctic in December (Figs. 4b, 4c). The simulated anticyclonic SLP anomaly and associated northerly cold air advection along its eastern flank are located further north and east (Fig. 4d) as compared with the reanalysis. For the combination of the AASIC loss and AMO+, the simulations do show the anomalous downward 150-hPa F_Z over the Siberia–Pacific sector, reduced blocking activity around the Caspian Sea, a below-normal snowpack over Western

Russia and Northern Europe and more widespread warming over the Arctic, Asia and Russia in December. Taken together, the ERA20CM simulations only partially represent the intensification (suppression) of the AASIC-related stratosphere–troposphere coupling during the wintertime in response to AMO− (AMO+), and do not well reproduce the horizontal winds at 10m (UV10) and tropospheric moisture transport.

Furthermore, we repeat a similar regression analysis as in Figs. 3 (c, d) and 4 (c, d), but without considering the phase of the AMO (Fig. S6). In connection with the AASIC loss, a southeastward-extended Eurasian snowpack and a "Warm Arctic, Cold Eurasia" pattern are still found in December, but weaker than those during the AMO−. In the simulations, we find a slightly thicker snowpack, while no significant cold continent anomaly over Eurasia, consistent with recent modeling studies [*McCusker et al.,* 2016; *Sun et al.,* 2016]. Hence, in a regression of ERA-I/ERA20CM, the sea ice impact irrespective of the phase of the AMO is weaker than the one inferred over the AMO− period. It points out the intermittency or state-dependence of the atmospheric response to sea ice [*Overland et al.,* 2016; *Smith et al.,* 2017].

4 Conclusions and Discussion

The influence of the interannual variability of AASIC decline on the stratosphere–troposphere coupling during different phases of the AMO is analyzed. When the AASIC loss combines with the AMO−, 1) there is increased Ural blocking activity and a thicker, southeastward-extended snowpack over Eurasia due to northerly cold advection and moisture transport from the Arctic, forming a pattern of "Warm Arctic, Cold Eurasia" in December. 2) Both the increased Ural blocking activity and the more-extended Eurasia snowpack favor upward 150-hPa F_Z anomalous over the Siberian–Pacific sector in the lower stratosphere. 3) The stratospheric polar vortex weakens, followed by a negative AO phase at the surface in February. When the AASIC loss combines with the AMO+, one finds more widespread warming over the Arctic and a reduced snowpack over Northern Eurasia in December, and the modulation of the stratosphere–troposphere coupling by sea ice during the wintertime is less important.

In the ERA20CM simulations with a state-of-the-art forecast model, the impact during

the AMO− is only partially recovered, despite the fact that it uses a higher horizontal resolution than that typically used in climate models. This indicates common, inter-related model issues like underestimated blocking activity, weak sensitivity to surface boundary forcing, or deficiencies in planetary wave propagation characteristics [*Handorf et al.,* 2015; *Overland et al.,* 2016; *Orsolini et al.,* 2016; *Smith et al.,* 2017].

Finally, the robustness of our findings concerning the AMO modulation of the impact of AASIC decline is further assessed by considering the whole twentieth century, using the AASIC index derived from NSIDC (Fig. S7: red bar) and the ERA20C reanalysis. During the AMO−, one finds a clear upward wave propagation over the Siberian–Pacific sector in December, an enhanced snowpack and cold anomaly over Southeastern Eurasia, and a negative AO pattern in February (Fig. S8: left panel) but with only a marginal increase in Ural blocking activity. These features are almost absent during the AMO+ (Fig. S8: right panel).

It is important to note that, within a decadal period of AMO−, the interannual varying AASIC means either sea ice loss or increase. By itself, the AMO− would act as an important background, inducing for example a stronger upper-tropospheric polar vortex. It is also acting to counter Arctic amplification (Figs. 2d, 2i), consistent with *Tokinaga et al.* [2017]. That is to say, in the mid to late twenty-first century when the AMO shifts to its cold phase with all other factors being equal, Arctic amplification might slowdown.

Acknowledgement

We acknowledge the Met Office Hadley Centre for making the observed global sea ice concentration data available, and ECMWF for the atmospheric reanalysis data. The HadISST2 dataset is available at https://www.metoffice.gov.uk/hadobs/hadisst2/. The ERA-I, ERA-I/Land, ERA20C and ERA20CM products are available from the ECMWF website [https://www.ecmwf.int/en/research/climate-reanalysis/browse-reanalysis-datasets]. This study was supported by the Research Council of Norway (Grant Nos. EPOCASA #229774/E10 and SNOWGLACE #244166), the National Key R&D Program of China (Grant No. 2016YFA0600703), the National Natural Science Foundation of China (Grant No. 41605059, 41505073 and 41375083), and the Young Talent Support Plan launched by the China

Association for Science and Technology (Grant No. 2016QNRC001). Comments and helpful suggestions from the editor and three anonymous reviewers helped us to improve the presentation of our results.

References

Årthun, M., T. Eldevik, L. H. Smedsrud, Ø. Skagseth, and R. B. Ingvaldsen (2012), Quantifying the influence of Atlantic heat on Barents Sea ice variability and retreat, *J. Clim., 25*(13), 4736–4743, doi:10.1175/JCLI-D-11-00466.1.

Balmaseda, M. A., L. Ferranti, F. Molteni, and T. N. Palmer (2010), Impact of 2007 and 2008 Arctic ice anomalies on the atmospheric circulation: Implications for long-range predictions, *Q. J. R. Meteorol. Soc., 136*, 1655–1664, doi:10.1002/qj.661.

Balsamo, G., et al. (2015), ERA-Interim/Land: a global land surface reanalysis data set, *Hydrol. Earth Syst. Sci., 19*(1), 389–407, doi:10.5194/hess-19-389-2015.

Cohen, J., M. Barlow, P. J. Kushner, and K. Saito (2007), Stratosphere–troposphere coupling and links with Eurasian land surface variability, *J. Clim., 20*(21), 5335–5343, doi:10.1175/2007JCLI1725.1.

Cohen, J., J. C. Furtado, M. A. Barlow, V. A. Alexeev, and J. E. Cherry (2012), Arctic warming, increasing snow cover and widespread boreal winter cooling. *Environ. Res. Lett., 7*(1), 014007, doi:10.1088/1748-9326/7/1/014007.

Cohen, J., J. Jones, J. C Furtado., and E. Tziperman (2013), Warm Arctic, cold continents: A common pattern related to Arctic sea ice melt, snow advance, and extreme winter weather, *Oceanography, 26*(4), 150–160, doi:10.5670/oceanog.2013.70.

Cohen, J., et al. (2014), Recent Arctic amplification and extreme mid-latitude weather, *Nat. Geosci., 7*(9), 627–637, doi:10.1038/ngeo2234.

Connolly, R., M. Connolly, and W. Soon (2017), Re-calibration of Arctic sea ice extent datasets using Arctic surface air temperature records, *Hydrolog. Sci. J., 62*(8), 1317–1340, doi:10.1080/02626667.2017.1324974.

Day, J. J., J. C. Hargreaves, J. D. Annan, , and A. Abe-Ouchi (2012), Sources of multi-decadal variability in Arctic sea ice extent. *Environ. Res. Lett., 7*(3), 034011, doi:10.1088/1748-9326/7/3/034011.

Dee, D. P., et al. (2011), The ERA- Interim reanalysis: Configuration and performance of the data assimilation system. *Q. J. R. Meteorol. Soc., 137*(656): 553–597, doi: 10.1002/qj.828.

Dima, M., and G. A Lohmann (2007), Hemispheric mechanism for the Atlantic Multidecadal

Oscillation. *J. Clim.*, *20*(11): 2706–2719, doi:10.1175/JCLI4174.1.

Enfield, D. B., A. M. Mestas-Nuñez, and P. J. Trimble (2001), The Atlantic Multidecadal Oscillation and its relationship to rainfall and river flows in the continental U.S., *Geophys. Res. Lett.*, *28*(10), 2077–2080, doi:10.1029/2000GL012745

Francis, J., and S. Vavrus (2012), Evidence linking Arctic amplification to extreme weather in mid-latitudes, *Geophys. Res. Lett.*, *39*(6), doi:10.1029/2012GL051000.

Gao, Y. Q., et al. (2015), Arctic sea ice and Eurasian climate: a review, *Adv. Atmos. Sci.*, *32*(1), 92–114, doi:10.1007/s00376-014-0009-6.

García-Herrera, R., and D. Barriopedro (2006), Northern Hemisphere snow cover and atmospheric blocking variability, *J. Geophys. Res.*, *111*, D21104, doi:10.1029/2005JD006975.

Gong, G., D. Entekhabi, and J. Cohen (2003), Modeled Northern Hemisphere winter climate response to realistic Siberian snow anomalies, *J. Clim.*, *16*(23), 3917–3931, doi:10.1175/1520-0442(2003)016<3917:MNHWCR>2.0.CO;2.

Handorf, D., R. Jaiser, K. Dethloff, A. Rinke, and J. Cohen (2015), Impacts of Arctic sea ice and continental snow cover changes on atmospheric winter teleconnections, *Geophys. Res. Lett.*, *42*(7), 2367–2377, doi:10.1002/2015GL063203.

Honda, M., J. Inoue, and S. Yamane (2009), Influence of low Arctic sea-ice minima on anomalously cold Eurasian winters. *Geophys. Res. Lett.*, *36*(8), doi:10.1029/2008GL037079.

Häkkinen, S., P. B. Rhines, and D. L. Worthen (2011), Atmospheric blocking and Atlantic Multidecadal Ocean variability, *Science*, *334*, 655–659, doi: 10.1126/science.1205683.

Hersbach, H., C. Peubey, A. Simmons, P. Berrisford, P. Poli, and D. Dee (2015), ERA-20CM: a twentieth-century atmospheric model ensemble, *Quart. J. Roy. Meteor. Soc.*, *141*(691), 2350–2375, doi: 10.1002/qj.2528.

Johannessen, O. M., et al. (2004), Arctic climate change: Observed and modelled temperature and sea-ice variability, *Tellus A*, *56*(4), 328–341, doi:10.1111/j.1600-0870.2004.00060.x.

Kim, B.-M., S.-W. Son, S.-K. Min, J.-H. Jeong, S.-J. Kim, X. Zhang, T. Shim, and J.-H. Yoon (2014), Weakening of the stratospheric polar vortex by Arctic sea-ice loss, *Nat.*

Commun., 5, 4646, doi:10.1038/ncomms5646.

King, M. P., M. Hell, and N. Keenlyside (2016), Investigation of the atmospheric mechanisms related to the autumn sea ice and winter circulation link in the Northern Hemisphere. *Clim. Dyn., 46*(3–4), 1185–1195, doi:10.1007/s00382-015-2639-5.

Kug, J.-S., J.-H. Jeong, Y.-S. Jang, B.-M. Kim, C. K. Folland, S.-K. Min, and S.-W. Son (2015), Two distinct influences of Arctic warming on cold winters over North America and East Asia, *Nat. Geosci., 8*(10), 759–762 (2015) doi:10.1038/ngeo2517.

Li, F., and H. J. Wang (2012), Autumn sea ice cover, winter Northern Hemisphere annular mode, and winter precipitation in Eurasia, *J. Clim., 26*(11), 3968–3981, doi:10.1175/JCLI-D-12-00380.1.

Li, F., Y. J. Orsolini, H. J. Wang, Y. Q. Gao, and S. P. He (2018), Modulation of the Aleutian--Icelandic low seesaw and its surface impacts by the Atlantic Multidecadal Oscillation, *Adv. Atmos. Sci., 35*(1), 95–105, doi:10.1007/s00376-017-7028-z.

Liu, J. P., J. A. Curry, H. J. Wang, M, Song, and R. M. Horton (2012), Impact of declining Arctic sea ice on winter snowfall, *Proc. Natl. Acad. Sci. USA, 109*(11), 4074–4079, doi: 10.1073/pnas.1114910109.

Mahoney, A. R., R. G. Barry, V. Smolyanitsky, and F. Fetterer (2008), Observed sea ice extent in the Russian Arctic, 1933–2006, *J. Geophys. Res., 113*, C11005, doi:10.1029/2008JC004830.

Miles, M. W., D. V. Divine, T. Furevik, E. Jansen, M. Moros, and A. E. J. Ogilvie (2014), A signal of persistent Atlantic multidecadal variability in Arctic sea ice, *Geophys. Res. Lett., 41*(2), 463–469, doi:10.1002/2013GL058084.

McCusker, K. E., J. C. Fyfe, and M. Sigmond (2016), Twenty-five winters of unexpected Eurasian cooling unlikely due to Arctic sea-ice loss, *Nat. Geosci., 9*(11), 838–842, doi:10.1038/ngeo2820.

Mori, M., M. Watanabe, H. Shiogama, J. Inoue, and M. Kimoto (2014), Robust Arctic sea-ice influence on the frequent Eurasian cold winters in past decades, *Nat. Geosci., 7*(12), 869–873, doi:10.1038/ngeo2277.

Nishii, K., H. Nakamura, and Y. J. Orsolini (2011), Geographical dependence observed in blocking high influence on the stratospheric variability through enhancement and

suppression of upward planetary-wave propagation, *J. Clim., 24*(24), 6408–6423, doi:10.1175/JCLI-D-10-05021.1.

Omrani, N.-E., N. S. Keenlyside, J. Bader, and E. Manzini (2014), Stratosphere key for wintertime atmospheric response to warm Atlantic decadal conditions, *Clim. Dyn., 42*, 649–663, doi:10.1007/s00382-013-1860-3.

Omrani, N.-E., J. Bader, N. S. Keenlyside, and E. Manzini (2016), Troposphere–stratosphere response to large-scale North Atlantic Ocean variability in an atmosphere/ocean coupled model. *Clim. Dyn., 46*(5-6): 1397–1415, doi:10.1007/s00382-015-2654-6.

Onarheim, I. H., L. H. Smedsrud, R. B. Ingvaldsen, and F. Nilsen (2014), Loss of sea ice during winter north of Svalbard, *Tellus A, 66*(1), 23933, doi:10.3402/tellusa.v66.23933.

Orsolini, Y. J., and N. G. Kvamstø (2009), Role of Eurasian snow cover in wintertime circulation: Decadal simulations forced with satellite observations, *J. Geophys. Res., 114*, D19108, doi:10.1029/2009JD012253.

Orsolini, Y. J., R. Senan, G. Balsamo, F. Doblas-Reyes, D. Vitart, A. Weisheimer, A. Carrasco, and R. Benestad (2013), Impact of snow initialization on sub-seasonal forecasts, *Clim. Dyn., 41*, 1969–1982, doi:10.1007/s00382-013-1782-0.

Orsolini, Y. J., R. Senan, F. Vitart, A. Weisheimer, G. Balsamo, and F. Doblas-Reyes (2016), Influence of the Eurasian snow on the negative North Atlantic Oscillation in subseasonal forecasts of the cold winter 2009/10, *Clim. Dyn. 47*(3), 1325–1334, doi:10.1007/s00382-015-2903-8.

Osborne, J. M., J. A. Screen, and M. Collins (2017), Ocean–atmosphere state dependence of the atmospheric response to Arctic sea ice loss, *J. Clim., 30*(5), 1537–1552, doi:10.1175/JCLI-D-16-0531.1.

Overland, J. E., et al. (2016), Nonlinear response of mid-latitude weather to the changing Arctic, *Nat. Clim. Change, 6*(11), 992–999, doi:10.1038/nclimate3121.

Peings, Y., D. Saint-Martin, and H. Douville (2012), A numerical sensitivity study of the influence of Siberian snow on the northern annular mode, *J. Clim., 25*(2): 592–607, doi:10.1175/JCLI-D-11-00038.1.

Peings, Y., and G. Magnusdottir (2014), Response of the wintertime Northern Hemisphere atmospheric circulation to current and projected Arctic sea ice decline: A numerical

study with CAM5, *J. Clim., 27*(1), 244–264, doi:10.1175/JCLI-D-13-00272.1.

Plumb, R. A. (1985), On the three-dimensional propagation of stationary waves, *J. Atmos. Sci., 42*(3), 217–229, doi:10.1175/1520-0469(1985)042<0217:OTTDPO>2.0.CO;2.

Poli, P., et al. (2016), ERA-20C: An atmospheric reanalysis of the twentieth century, *J. Clim., 29*(11), 4083–4097, doi:10.1175/JCLI-D-15-0556.1.

Saito, K., J, Cohen, and D. Entekhabi (2001), Evolution of atmospheric response to early-season Eurasian snow cover anomalies, *Mon. Weather Rev., 129*(11), 2746–2760, doi:10.1175/1520-0493(2001)129<2746:EOARTE>2.0.CO;2.

Schlesinger, M. E., and N. Ramankutty (1994), An oscillation in the global climate system of period 65-70 years, *Nature, 367*(6465), 723–726, doi: 10.1038/367723a0.

Screen, J. A. (2017), The missing Northern European winter cooling response to Arctic sea ice loss, *Nat. Commun., 8*, 14603, doi:10.1038/ncomms14603.

Smith, D. M., N. J. Dunstone, A. A. Scaife, E. K. Fiedler, D. Copsey, and S. C. Hardiman (2017), Atmospheric response to Arctic and Antarctic sea ice: The importance of ocean-atmosphere coupling and the background state, *J. Clim., 30*(12), 4547–4565, doi:10.1175/JCLI-D-16-0564.1.

Stroeve, J. C., M. C. Serreze, M. M. Holland, J. E. Kay, J. Malanik, and A. P. Barrett (2012), The Arctic's rapidly shrinking sea ice cover: a research synthesis, *Climatic Change, 110*(3–4), 1005–1027, doi:10.1007/s10584-011-0101-1.

Sun, L., J. Perlwitz, and M. Hoerling (2016), What caused the recent "Warm Arctic, Cold Continents" trend pattern in winter temperatures?, *Geophys. Res. Lett., 43*(10), 5345–5352, doi:10.1002/2016GL069024.

Tang, Q., X. Zhang, X. Yang, and J. Francis (2013), Cold winter extremes in northern continents linked to Arctic sea ice loss, *Environ. Res. Lett., 8*(1), 014036, doi:10.1088/1748-9326/8/1/014036.

Thompson, D. W. J, and J. M. Wallace (2001), Regional climate impacts of the Northern Hemisphere annular mode, *Science, 293*(5527), 85–89, doi:10.1126/science.1058958.

Titchner, H. A., and N. A. Rayner (2014), The Met Office Hadley Centre sea ice and sea surface temperature data set, version 2: 1. Sea ice concentrations, *J. Geophys. Res.*

Atmos., *119*(6), 2864–2889, doi:10.1002/2013JD020316.

Tokinaga, H., S. P. Xie, and H. Mukougawa (2017), Early 20th-century Arctic warming intensified by Pacific and Atlantic multi-decadal variability, *Proc. Natl. Acad. Sci. USA*, *114*(24), 6227–6232, doi:10.1073/pnas.1615880114.

Vihma, T. (2014), Effects of Arctic sea ice decline on weather and climate: a review, *Surv. Geophys.*, *35*(5), 1175–1214, doi:10.1007/s10712-014-9284-0.

Walsh, J. E., F. Fetterer, J. S. Stewart, and W. L. Chapman (2017), A database for depicting Arctic sea ice variations back to 1850, *Geogr. Rev.*, *107*(1), 89–107, doi:10.1111/j.1931-0846.2016.12195.x.

Wegmann, M., et al. (2015), Arctic moisture source for Eurasian snow cover variations in autumn, *Environ. Res. Lett.*, *10*(5), 054015, doi:10.1088/1748-9326/10/5/054015.

Zhang, R. (2015), Mechanisms for low-frequency variability of summer Arctic sea ice extent, *Proc. Natl. Acad. Sci. USA*, *112*(15), 4570–4575, doi:10.1073/pnas.1422296112.

Zhang, J., W. Tian, M. P. Chipperfield, F. Xie, and J. Huang (2016), Persistent shift of the Arctic polar vortex towards the Eurasian continent in recent decades, *Nat. Clim. Change*, *6*(12), 1094–1099, doi:10.1038/nclimate3136.

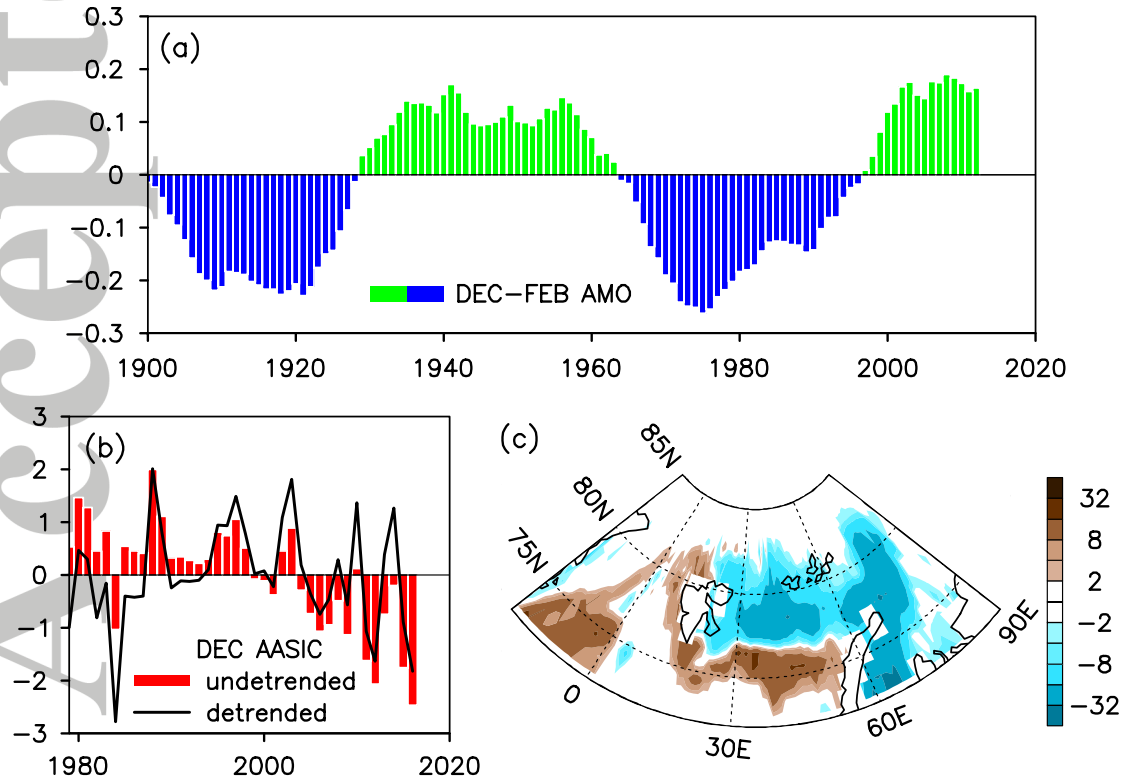

Figure 1 (**a**) Time evolution of the smoothed December–February mean AMO index for 1900/01–2011/12. (**b**) Time evolution of the undetrended (red bar) and detrended (black line) December AASIC index for 1979–2016. (**c**) The decadal difference of the standard deviation (unit: %) of December sea ice concentration between 1979–1995 and 1996–2016 (1979–1995 minus 1996–2016).

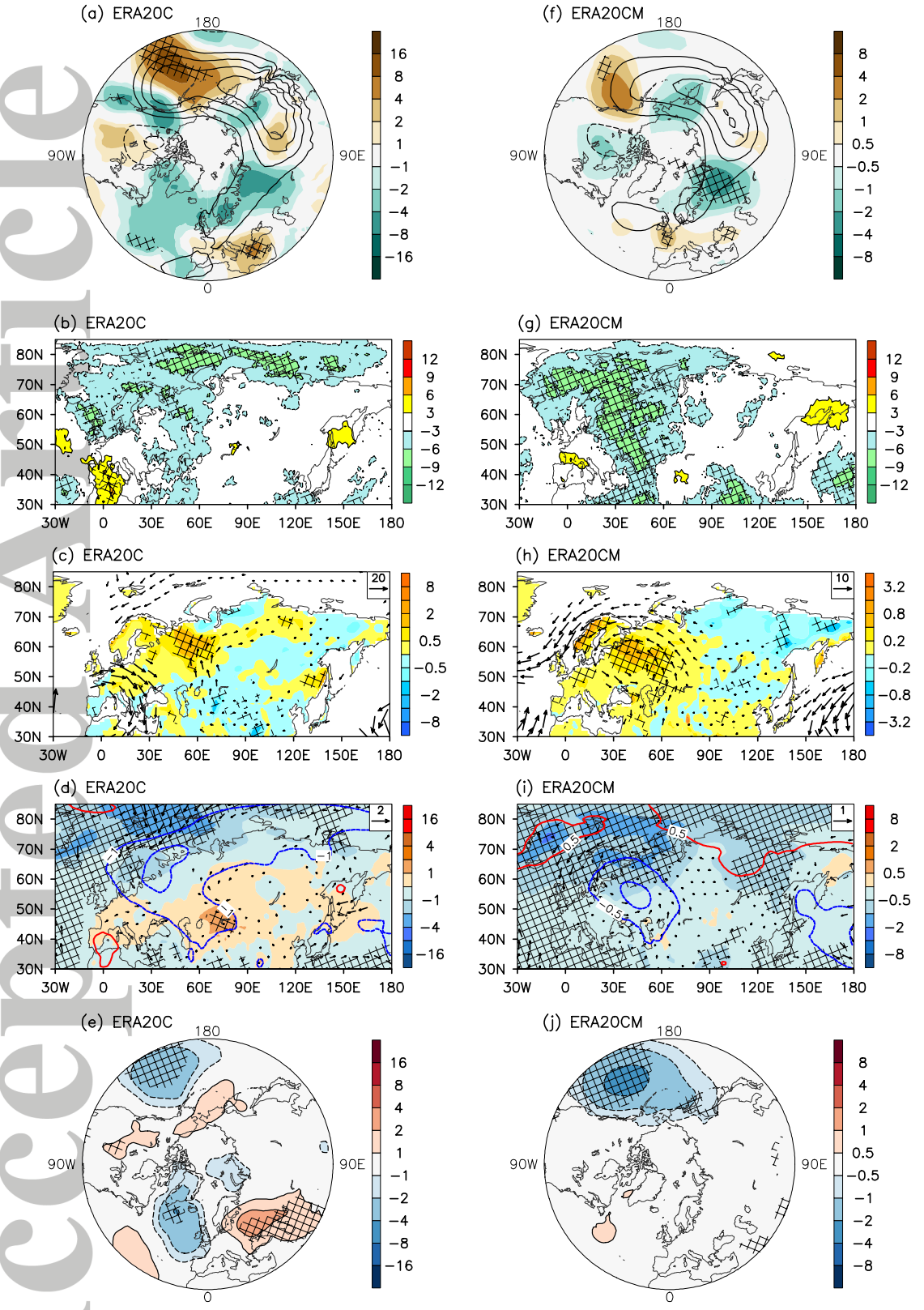

Figure 2 (**a**) The climatology (contours; interval: 10^{-2} m^2 s^{-2}) and composite difference (shaded; unit: 10^{-3} m^2 s^{-2}) between the AMO− and AMO+ (AMO− minus AMO+) of December 150-hPa Fz. The composite difference between the AMO− and AMO+ of (**b**) the frequency of blocking heights (unit: %), (**c**) Eurasian snow depth (shaded; unit: mm)

and integrated water vapour transport (vectors; unit: kg m^{-1} s^{-1}), (**d**) SLP (contours; unit: hPa)/UV10m (vectors; unit: m s^{-1})/TS (shaded; unit: °C) in December and (**e**) SLP (unit: hPa) in February. Those values exceeding 95% confidence interval are denoted by slash. *The datasets are derived from ERA20C (1900/01–2009/2010).* (**f–j**) As in (a–e), except for *ERA20CM (1900/01–2009/2010)*, using a different color scale.

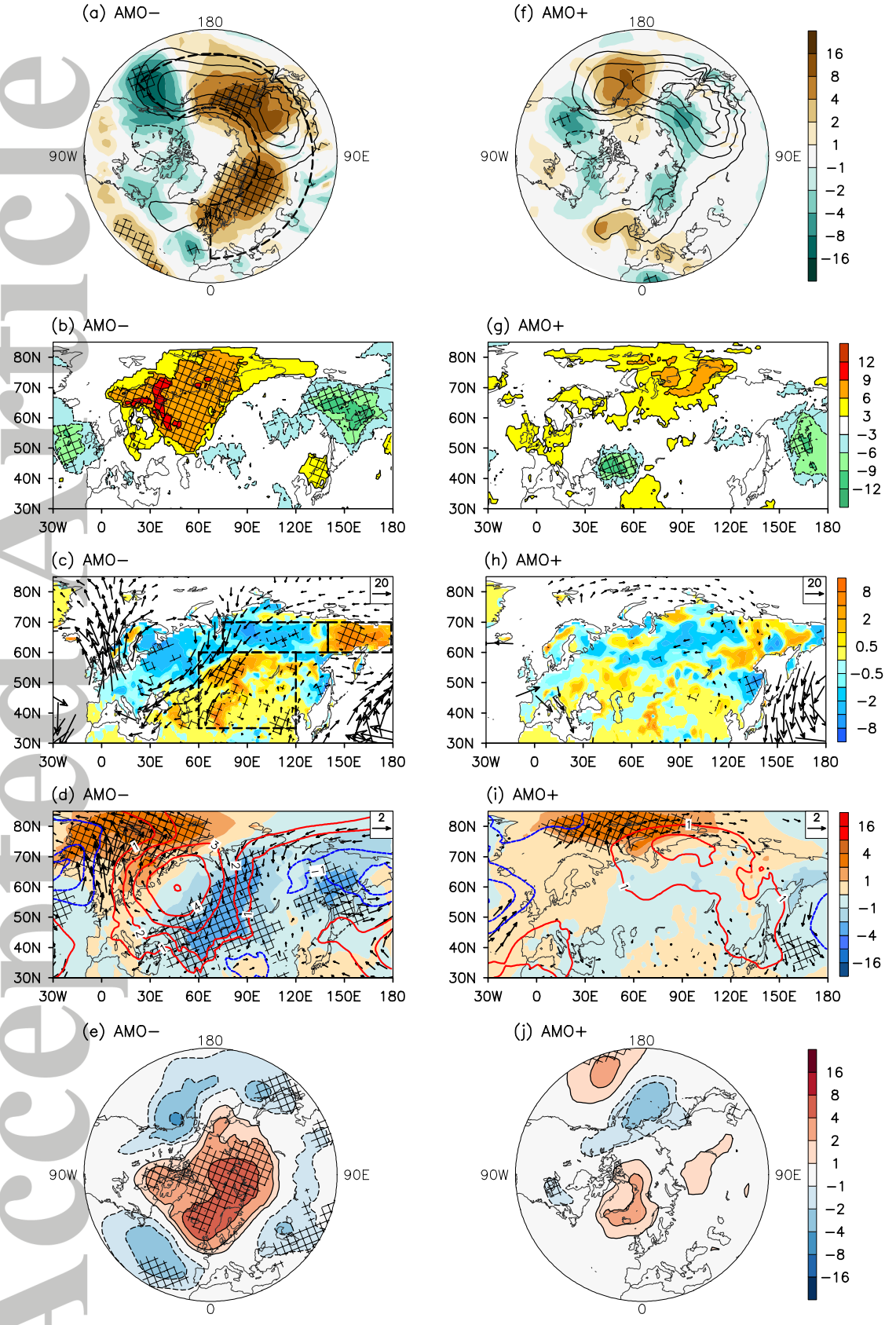

Figure 3 (**a**) The climatology (contours; interval: 10^{-2} m^2 s^{-2}) and regression (shaded; unit: 10^{-3} m^2 s^{-2}) upon the negative AASIC index for the AMO− period of December 150-hPa

F_Z. The regression upon the negative AASIC index for the AMO− period of (**b**) the frequency of blocking heights (unit: %), (**c**) Eurasian snow depth (shaded; unit: mm) and integrated water vapour transport (vectors; unit: kg m^{-1} s^{-1}), (**d**) SLP (contours; unit: hPa)/UV10m (vectors; unit: m s^{-1})/TS (shaded; unit: °C) in December and (**e**) SLP (unit: hPa) in February. Those values exceeding 95% confidence interval are denoted by slash. (**f–j**) As in (a–e), except for the AMO+ period. *The datasets are derived from ERA-I (1979/80–2016/17) and ERA-I/Land (1980–2014).* The black frames in Fig. 3a and 3c depict the regions used to define F_Z and ESD indices, respectively (see Supplementary).

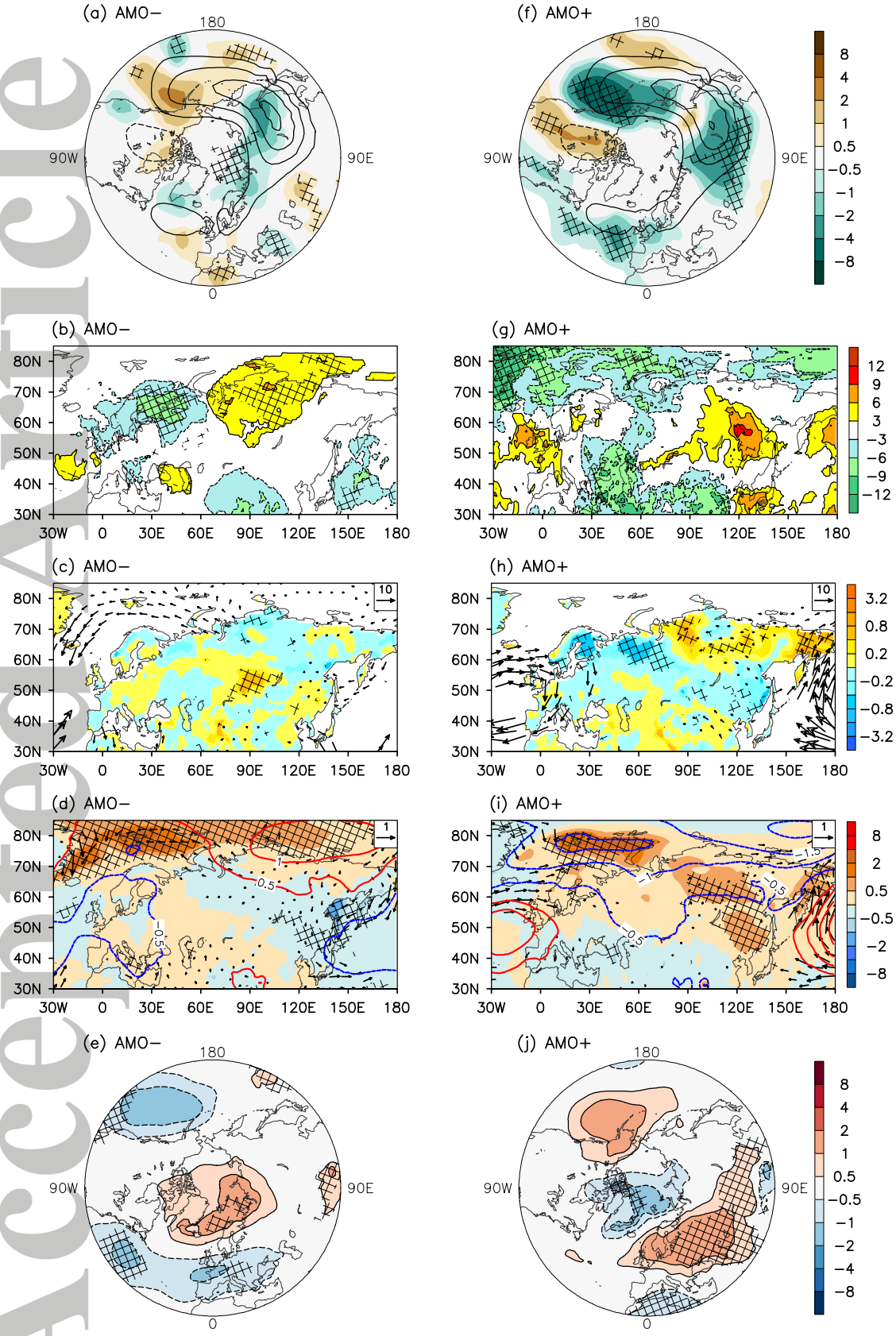

Figure 4 As in Fig. 3, except for *ERA20CM (1979/80–2009/10).* Those values exceeding 90% confidence interval are denoted by slash.